Hindawi Publishing Corporation
Mathematical Problems in Engineering
Volume 2012, Article ID 710586, 16 pages
doi:10.1155/2012/710586

Research Article

Phase Error Modeling and Its Impact on Precise Orbit Determination of GRACE Satellites

Jia Tu,[1,2] Defeng Gu,[2] Yi Wu,[2] Dongyun Yi,[2] and Jiasong Wang[1]

[1] *State Key Laboratory of Astronautic Dynamics, Xi'an 710043, China*
[2] *Department of Mathematics and Systems Science, College of Science, National University of Defense Technology, Changsha 410073, China*

Correspondence should be addressed to Jia Tu, tu_jia_jia@yahoo.com.cn

Received 31 March 2012; Revised 11 July 2012; Accepted 17 July 2012

Academic Editor: Serge Prudhomme

Limiting factors for the precise orbit determination (POD) of low-earth orbit (LEO) satellite using dual-frequency GPS are nowadays mainly encountered with the in-flight phase error modeling. The phase error is modeled as a systematic and a random component each depending on the direction of GPS signal reception. The systematic part and standard deviation of random part in phase error model are, respectively, estimated by bin-wise mean and standard deviation values of phase postfit residuals computed by orbit determination. By removing the systematic component and adjusting the weight of phase observation data according to standard deviation of random component, the orbit can be further improved by POD approach. The GRACE data of 1–31 January 2006 are processed, and three types of orbit solutions, POD without phase error model correction, POD with mean value correction of phase error model, and POD with phase error model correction, are obtained. The three-dimensional (3D) orbit improvements derived from phase error model correction are 0.0153 m for GRACE A and 0.0131 m for GRACE B, and the 3D influences arisen from random part of phase error model are 0.0068 m and 0.0075 m for GRACE A and GRACE B, respectively. Thus the random part of phase error model cannot be neglected for POD. It is also demonstrated by phase postfit residual analysis, orbit comparison with JPL precise science orbit, and orbit validation with KBR data that the results derived from POD with phase error model correction are better than another two types of orbit solutions generated in this paper.

1. Introduction

Since spaceborne dual-frequency Global Positioning System (GPS) receiver was successfully applied in CHAllenging Minisatellite Payload (CHAMP) mission [1, 2], more and more low-earth orbit (LEO) satellite missions have been equipped with dual-frequency GPS receiver for precise navigation, such as Gravity Recovery And Climate Experiment (GRACE) mission [3], Gravity field and steady-state Ocean Circulation Explorer (GOCE) mission [4], and TanDEM-X mission [5]. Due to the characteristic of good continuity, high precision, and low cost,

the spaceborne dual-frequency GPS receiver has become a primary instrument for precise orbit determination (POD) of LEO satellite. By the processing of GPS observation data, 3dimensional (3D) in-flight position information of satellite can be obtained with centimeter-level precision [6–8].

At present, the reduced dynamic orbit determination method [8–10] is widely used for LEO POD based on dual-frequency GPS, which combines the geometric strength of the GPS observations with the orbit dynamical model constraints. In this way, the available accuracy of the GPS measurements may be fully exploited without sacrificing the robustness offered by dynamic orbit determination techniques. Thanks to numerous improvements in the final GPS orbit and clock products provided by the International GNSS Service (IGS) [11], in the orbit dynamical models of LEO satellite, and in the approaches of data processing and orbit determination, the accuracy of LEO POD based on dual-frequency GPS can be steadily improved.

Note that the noise level of GPS carrier phase measurement of GPS receiver can reach 1-2 mm, which is much more accurate than GPS pseudo code observation. Therefore, the quality of phase observation will directly determine the accuracy of LEO POD. However, there exist different kinds of errors in the phase observation, such as phase measurement error, receiver antenna phase center location error, and near-field multipath. The phase error belongs to mixed error formed by random error and systematic error, and the error character is complex. Therefore, the researches on phase error modeling and correction provide a valid way to further improve the precision of orbit determination. The residual approach [7, 12–15] is a widely used method for in-flight calibrations of phase errors. In this approach, calibrations are derived as bin-wise mean values from GPS carrier phase postfit residuals obtained from orbit determination. The JASON-1 orbits [12] have already been successfully improved by this approach. Meanwhile, the Jet Propulsion Laboratory (JPL) [13] applies this approach to the GRACE satellites, which serves as primary data source to derive phase center variations (PCVs) for the GPS transmitter antennas. In addition, Montenbruck et al. [14], Jäggi et al. [7], and Bock et al. [15] use this approach to calibrate the PCVs of GPS receiver antennas onboard GRACE, TerraSAR-X, and GOCE, respectively. In this approach, only bin-wise mean values of phase postfit residuals are considered for the in-flight calibrations, and the systematic part in phase error can be partly calibrated. However, the random part is less considered, that is, the bin-wise standard deviation information of phase postfit residuals is neglected.

Subsequently, we mainly focus on the whole modeling of phase error and assess its impact on GRACE POD. In this paper, the phase error is modeled as a systematic and a random component each depending on the direction of signal reception. The systematic part and the standard deviation of random part in the direction of signal reception are, respectively, estimated. The final LEO orbit can be determined by removing the systematic part and adjusting the weight of phase data. For this investigation, the GRACE satellites are selected. The GRACE mission [3], launched on March 17, 2002, is a joint partnership between the National Aeronautics and Space Administration (NASA) in the United States and Deutsches Zentrum für Luft-und Raumfahrt (DLR) in Germany. It consists of two identical formation flying spacecraft (GRACE A and GRACE B) in a near polar, near circular orbit with an initial altitude of about 500 km. The spacecraft has a nominal separation of 220 km. The key science instruments onboard both spacecraft include a BlackJack GPS receiver, a SuperSTAR accelerometer, a star tracker, a K-band ranging (KBR) system, and a satellite laser ranging (SLR) retroreflector. The BlackJack GPS receiver exhibits a representative noise level of 1 mm for $L1$ and $L2$ carrier phase measurements.

Section 2 focuses on the in-flight phase error modeling, parameter estimation of error model, and POD with phase error correction. In Section 3, the phase error model is applied to the real GPS observation data of GRACE and its impact on POD is discussed. Section 4 shows the conclusions.

2. In-Flight GPS Phase Error Modeling

2.1. Observation Equation

In order to eliminate the first order ionosphere delay, dual-frequency ionosphere-free combination observations are always adopted. For the pseudocode and carrier phase observations, the ionosphere-free combination yields

$$P_{\mathrm{IF}}^{j}(t) = \frac{f_1^2}{f_1^2 - f_2^2} \cdot P_1^j(t) - \frac{f_2^2}{f_1^2 - f_2^2} \cdot P_2^j(t) = \rho^j\left(t, \tau^j\right) + c \cdot \delta t(t) + \delta\rho_{\mathrm{cor}}(t), \tag{2.1}$$

$$L_{\mathrm{IF}}^{j}(t) = \frac{f_1^2}{f_1^2 - f_2^2} \cdot L_1^j(t) - \frac{f_2^2}{f_1^2 - f_2^2} \cdot L_2^j(t) = \rho^j\left(t, \tau^j\right) + c \cdot \delta t(t) + b_{\mathrm{IF}}^{j} + \delta\rho_{\mathrm{cor}}(t), \tag{2.2}$$

where subscript "IF" denotes ionosphere-free combination, subscripts 1 and 2 denote different frequencies, P_{IF} is pseudo code ionosphere-free combination, L_{IF} is phase ionosphere-free combination, f_i is the carrier frequency, τ^j is the real signal traveling time from GPS satellite j to LEO satellite which can be obtained by iterative calculation, $\rho^j(t, \tau^j)$ is geometric distance between the mass center position of GPS satellite j and LEO satellite at signal transmission epoch $t - \tau^j$ and signal reception epoch t, respectively, and c is light velocity. δt is the clock offset of LEO satellite, b_{IF} is the ambiguity of phase ionosphere-free combination, and $\delta\rho_{\mathrm{cor}}$ is a series of corrections which can be denoted as

$$\delta\rho_{\mathrm{cor}}(t) = -c \cdot \delta\rho_{\mathrm{clk}}\left(t, \tau^j\right) + \delta\rho_{\mathrm{rel}}(t) + \delta\rho_{\mathrm{GPS}}^{j}(t) + \delta\rho_{\mathrm{LEO}}(t), \tag{2.3}$$

where $\delta\rho_{\mathrm{clk}}$ is the clock correction of GPS satellite j at epoch $t - \tau^j$, $\delta\rho_{\mathrm{rel}}$ is the relativity correction of GPS satellite j, $\delta\rho_{\mathrm{GPS}}$ is the phase center offset correction of GPS satellite j, and $\delta\rho_{\mathrm{LEO}}$ is the ionosphere-free phase center correction of LEO satellite. These corrections have been studied by other scholars [16] and are not discussed in this paper.

For convenience, $\rho^j(t, \tau^j)$ has to be linearized as

$$\rho^j\left(t, \tau^j\right) = \rho_0^j\left(t, \tau^j\right) - \left(\mathbf{e}^j(t)\right)^T \cdot \Delta\mathbf{r}(t), \tag{2.4}$$

where

$$\begin{aligned} \rho_0^j\left(t, \tau^j\right) &= \left\|\mathbf{r}^j\left(t - \tau^j\right) - \mathbf{r}_0(t)\right\|, \\ \Delta\mathbf{r}(t) &= \mathbf{r}(t) - \mathbf{r}_0(t), \\ \mathbf{e}^j(t) &= \frac{\mathbf{r}^j\left(t - \tau^j\right) - \mathbf{r}_0(t)}{\left\|\mathbf{r}^j\left(t - \tau^j\right) - \mathbf{r}_0(t)\right\|}, \end{aligned} \tag{2.5}$$

where $\mathbf{r}^j(t-\tau^j)$ is the mass center position of GPS satellite j in conventional inertial reference frame (CIRF) at epoch $t-\tau^j$, $\mathbf{r}_0(t)$ is the approximate mass center position of LEO satellite in CIRF, and $\mathbf{e}^j(t)$ is a line of sight (LOS) vector.

2.2. Phase Error Modeling

For the convenience of description, the definition of Antenna-Fixed Coordinate System (AFCS) [14] is given at first. The origin O is mechanical antenna reference point (ARP). The positive Z-axis coincides with the mechanical symmetry axis and points along the boresight direction. The Y-axis and X-axis point from the mechanical ARP into the respective directions, which depend on the specific mounting of the antennas. Take AFCS of GRACE satellites for instance. The X-axis of AFCS coincides with x-axis of Satellite Body Coordinate System (SBCS). The Y-axis of AFCS is in opposite direction with y-axis of SBCS and Z-axis of AFCS completes a right-handed coordinate system. In AFCS, the azimuth angle of a vector $\mathbf{r}$ is defined as an angle between the projection of $\mathbf{r}$ in XOY-plane and positive X-axis and is counted in a counter-clockwise sense from the X-axis to the Y-axis. The elevation angle of a vector $\mathbf{r}$ is defined as an angle between $\mathbf{r}$ and XOY-plane.

As the in-flight GPS phase error consists of GPS receiver antenna phase center location error, phase observation error, near-field multipath, and all other nonmodeled phase errors, it can be composed of systematic part and random part, which both depend on the direction of GPS signal reception. Assuming that the LOS vector of GPS reception signal in CIRF is $\mathbf{e}^j$, the phase error $\varepsilon_i(\mathbf{e}^j)$ on Li $(i=1,2)$ band along this direction can be modeled as

$$\varepsilon_i\left(\mathbf{e}^j\right) = \varepsilon_{S,i}\left(\mathbf{e}^j\right) + \varepsilon_{R,i}\left(\mathbf{e}^j\right), \quad i=1,2, \tag{2.6}$$

where $\varepsilon_{S,i}(\mathbf{e}^j)$ and $\varepsilon_{R,i}(\mathbf{e}^j)$ are the systematic part and random part of phase, respectively, $\varepsilon_{R,i}(\mathbf{e}^j)$ is a random variable from normal distribution $N(0,\sigma_i^2(\mathbf{e}^j))$ with mean value of 0 and standard deviation of $\sigma_i(\mathbf{e}^j)$, and $\varepsilon_{R,i}(\mathbf{e}^j)$ and $\varepsilon_{R,i}(\mathbf{e}^k)$ are independent if $\mathbf{e}^j \neq \mathbf{e}^k$.

From (2.6), the ionosphere-free phase error model can be expressed as

$$\varepsilon_{\mathrm{IF}}\left(\mathbf{e}^j\right) = \alpha_1 \cdot \varepsilon_1\left(\mathbf{e}^j\right) - \alpha_2 \cdot \varepsilon_2\left(\mathbf{e}^j\right) = \varepsilon_{S,\mathrm{IF}}\left(\mathbf{e}^j\right) + \varepsilon_{R,\mathrm{IF}}\left(\mathbf{e}^j\right). \tag{2.7}$$

2.3. Parameter Estimation of Phase Error Model

Assuming that the GPS ionosphere-free carrier phase observation value at epoch t is $z_{\mathrm{IF}}^j(t)$, LOS vector is $\mathbf{e}^j(t)$, and the ionosphere-free phase observation model value from (2.2) is $L_{\mathrm{IF}}^j(t)$, then the ionosphere-free phase error value can be expressed as

$$\varepsilon_{\mathrm{IF}}\left(\mathbf{e}^j(t)\right) = z_{\mathrm{IF}}^j(t) - L_{\mathrm{IF}}^j(t). \tag{2.8}$$

From (2.8), the ionosphere-free phase error can be directly estimated by the postfit residuals of orbit determination. The LEO orbits can be directly obtained by reduced dynamic orbit determination approach. As the phase error depends on the direction of GPS reception signal, that is, the azimuth angle and elevation angle of the LOS vector in AFCS, phase error

can be estimated by azimuth/elevation bins. In this study, the phase postfit residuals are sorted in azimuth/elevation bins of $\Delta A \times \Delta E$. The mean value E_{nm} and standard deviation σ_{nm} of all the phase postfit residuals fallen into the region of $[(n-1)\cdot\Delta A, n\cdot\Delta A)\times[(m-1)\cdot\Delta E, m\cdot\Delta E)$, $(n=1,2,\ldots,360^\circ/\Delta A; m=1,2,\ldots,90^\circ/\Delta E)$ are obtained. The values of ΔA and ΔE are both selected as 5° in this paper. If the azimuth angle and elevation angle of the LOS vector $\mathbf{e}^j(t)$ are fallen into the region of $[(n-1)\cdot\Delta A, n\cdot\Delta A)\times[(m-1)\cdot\Delta E, m\cdot\Delta E)$, E_{nm} is selected as the estimation of phase systematic part $\varepsilon_{S,\mathrm{IF}}(\mathbf{e}^j(t))$ and σ_{nm} is the estimation of standard deviation $\sigma_{\mathrm{IF}}(\mathbf{e}^j)$ of phase random part $\varepsilon_{R,\mathrm{IF}}(\mathbf{e}^j(t))$. They are denoted as follows:

$$\begin{aligned}\widehat{\varepsilon}_{S,\mathrm{IF}}\left(\mathbf{e}^j(t)\right) &= E_{nm},\\ \widehat{\sigma}_{\mathrm{IF}}\left(\mathbf{e}^j(t)\right) &= \sigma_{nm}.\end{aligned} \tag{2.9}$$

2.4. POD with Phase Error Correction

From (2.8) and (2.9), we can get

$$z^j_{\mathrm{IF}}(t) - L^j_{\mathrm{IF}}(t) - E_{nm} = \varepsilon_{\mathrm{IF}}\left(\mathbf{e}^j(t)\right) - \widehat{\varepsilon}_S\left(\mathbf{e}^j(t)\right) \sim N\left(0, \sigma^2_{nm}\right). \tag{2.10}$$

According to (2.10), the orbit parameters can be improved by reduced dynamic orbit determination approach in a second step after removing the systematic part and adjusting the weight of phase observation data according to σ_{nm}.

Assuming that the phase outliers have been removed, the elevation cutoff angle is E_0 (= 5°), the azimuth angle and elevation angle of phase observation data are A and E, respectively, the standard deviation of all the phase postfit residuals is σ_0, and the weights of phase observation data are set as follows.

(1) If $E < E_0$, the weight of phase observation data is 0.

(2) When $E \geq E_0$, A and E are fallen into the region of $[(n-1)\cdot\Delta A, n\cdot\Delta A)\times[(m-1)\cdot\Delta E, m\cdot\Delta E)$, if $\sigma_{nm} > 0$, the weight of phase observation data is $(\sigma_0/\sigma_{nm})^2$, if $\sigma_{nm} = 0$, the weight of phase observation data is 0.

The flow of data processing for LEO POD is shown in Figure 1.

3. Numerical Analysis for GRACE Satellites

3.1. Data Sets and Processing Strategies

The data sets used here include GPS observation data (GPS1B), spacecraft attitude data (SCA1B), KBR data (KBR1B), JPL precise science orbit data (GNV1B) of GRACE A and GRACE B [17] from GeoForschungsZentrum (GFZ), and the final GPS orbits and the 30 s high-rate satellite clock corrections from the Center for Orbit Determination in Europe (CODE) [18]. The data cover a period of 31 days from January 1 to January 31 of 2006. The phase center offsets of GPS receiver antennas onboard GRACE satellites [19] in respective SBCS are listed in Table 1.

The LEO orbit determination is implemented in the separate software tools as part of the NUDT Orbit Determination Software 1.0. The GPS observation data processing consists

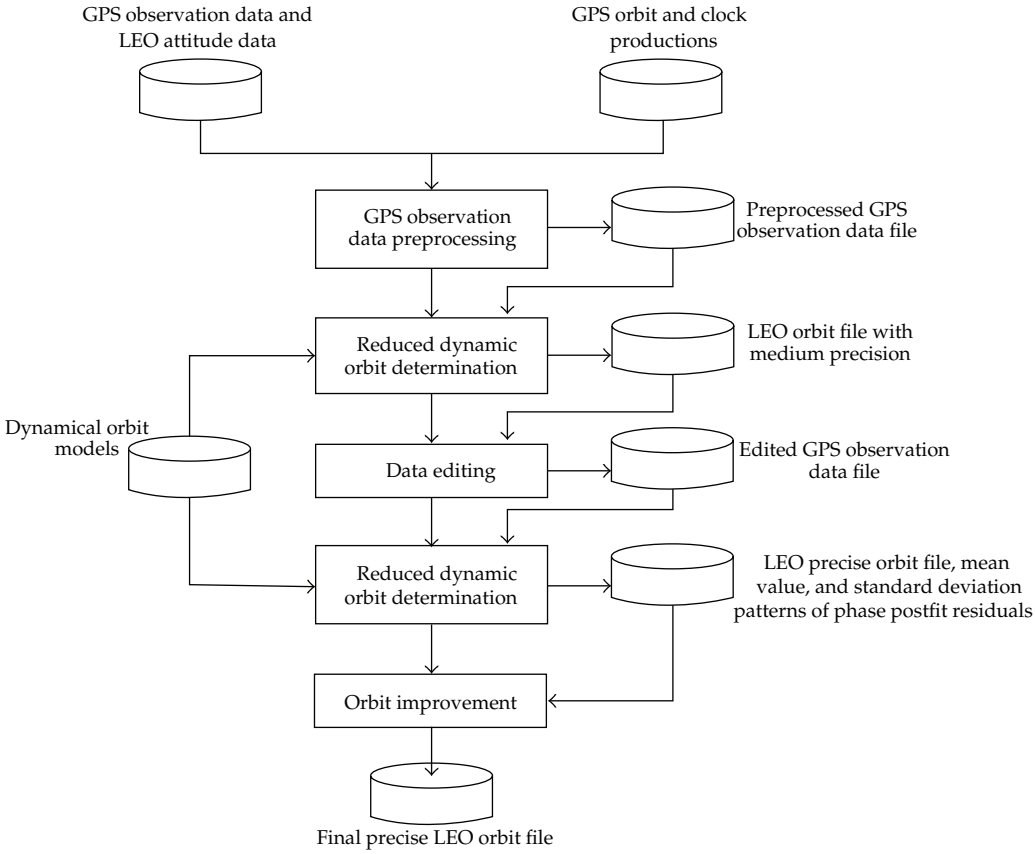

Figure 1: Flow of data processing for precise orbit determination.

Table 1: Phase center offsets of GPS receiver antennas onboard GRACE satellites in the respective SBCS.

	x (m)	y (m)	z (m)
GRACE A	0.0004	−0.0004	−0.4140
GRACE B	0.0006	−0.0008	−0.4143

of GPS observation data preprocessing [16], reduced dynamic orbit determination with medium precision [16, 19], GPS observation data editing [16, 19], and reduced dynamic orbit determination with high precision. Both reduced dynamic orbit determinations with medium and high precision make use of zero-difference (ZD) reduced dynamic batch Least-SQuares (LSQ) approach. In this approach, the individual spacecraft positions at each measurement epoch are replaced by the spacecraft trajectory model in (2.1) and (2.2). We make use of known physical models of the spacecraft motion to constrain the resulting position estimates and introduce three empirical acceleration components to absorb all other nonmodeled perturbation. As the atmospheric density and solar activity are difficult to model accurately, atmospheric drag coefficient and solar radiation pressure coefficient in the models of atmospheric drag and solar radiation pressure are also estimated. The orbit dynamical models and reference frames used for reduced dynamic orbit determination are listed in Table 2.

Table 2: Overview of the dynamical models and reference frames used for reduced dynamic orbit determination.

Item	Description
Static gravity field	GGM02C 150 × 150 [20]
Solid Earth tide	IERS96, 4 × 4 [21]
Polar tide	IERS96 [21]
Ocean tide	CSR4.0
3rd body gravity	Sun and moon
Solar radiation pressure	Ball model, Conical earth shadow, C_R is estimated [22]
Atmospheric drag	Jacchia 71 density model (NOAA solar flux (daily) and geomagnetic activity (3 hourly)), C_D is estimated [22]
Relativity	Schwarzschild
Precession	IAU1976 [21]
Nutation	IAU1980 + EOPC correction [21]
Earth orientation	EOPC04
Solar ephemerides	JPL DE405
Terrestrial reference frame	International Terrestrial Reference Frame (ITRF) 2000 [23]
Conventional inertial reference frame	J2000.0 [24]

Table 3: Parameters estimated in orbit determination.

Estimated parameter	Description
Initial state vector	3D position and velocity estimated per day
Atmospheric drag coefficient	Estimated per 3 hour
Solar radiation pressure coefficient	Estimated per 12 hours
Empirical acceleration coefficient	c_r, s_r, c_t, s_t, c_n, s_n estimated per orbital revolution
LEO clock offset	Estimated epoch-wise
Ambiguity	Estimated per arc of continuous tracking of a single GPS satellite

Three empirical acceleration components in the radial (R), transverse (T) and normal (N) direction are denoted as [25]

$$\mathbf{a}_{RTN} = \begin{bmatrix} c_r \cdot \cos u + s_r \cdot \sin u \\ c_t \cdot \cos u + s_t \cdot \sin u \\ c_n \cdot \cos u + s_n \cdot \sin u \end{bmatrix} \cdot \begin{bmatrix} \mathbf{e}_R \\ \mathbf{e}_T \\ \mathbf{e}_N \end{bmatrix}, \tag{3.1}$$

where u is satellite latitude, c_r, s_r, c_t, s_t, c_n, and s_n are empirical acceleration coefficients, and $\mathbf{e}_R$, $\mathbf{e}_T$, and $\mathbf{e}_N$ are unit vectors in directions of R, T, and N, which are three axes of RTN coordinate system.

All the parameters are estimated by batch LSQ approach [16, 19]. The parameters estimated in orbit determination are listed in Table 3. Orbit determination process is typically conducted in 24-hour data batches, and Adams-Cowell multistep integration method [26] is used for orbit integration.

3.2. Parameter Estimation Results Adopting Phase Error Model

At first, all the GPS observation data of GRACE A and GRACE B are processed to obtain the orbits using POD without phase error model correction. The mean values and standard deviations of phase postfit residuals are stored with a resolution of 5° × 5°. The mean value patterns and standard deviation patterns of GRACE satellites are shown in Figure 2. It is shown by Figure 2 that the mean value patterns and standard deviation patterns of both satellites exhibit the similar distributions. In addition, it is shown by mean value patterns and standard deviation patterns from different periods that the distributions of mean value patterns and standard deviation patterns keep relatively steady and can be assumed to keep constant with time.

3.3. Impact of Phase Error Modeling on GRACE POD

In this section, besides the GRACE orbit solutions computed by POD without phase error model correction as mentioned in Section 3.2, another two types of GRACE orbit solutions derived from POD with mean value correction of phase error model and POD with phase error model correction are also analyzed. The mean value correction of phase error model is just the residual approach. Phase postfit residual analysis, orbit comparison, and orbit validation with KBR data are used to analyze the impact of phase error modeling on GRACE POD.

3.3.1. Phase Postfit Residual Analysis

Phase postfit residual analysis can be used to measure the consistency of the applied models with the GPS observation data. The Root Mean Square (RMS) errors of ionosphere-free phase postfit residuals of POD are shown in Table 4.

It is found by statistic results that the mean values of phase postfit residuals are close to 0 m (see Figure 3). From Table 4, the RMS values of phase postfit residuals derived from POD with phase error model correction are 9.96 mm for GRACE A and 9.28 mm for GRACE B, which are less than those computed by POD without phase error model correction and POD with only mean value correction of phase error model. It is shown by these results that the applied models are in better consistency with GPS observation data using POD with phase error model correction.

3.3.2. Orbit Comparison

In an effort to obtain some information on the orbit improvement arisen from phase error model correction and the quality of GRACE orbits computed in this paper, internal and external quality metrics are used for orbit comparison. The sampling intervals of orbits are 30 s. In internal quality metric, the orbits generated by POD with phase error model correction (identifier "POD + PMC") are compared with the orbits obtained by POD without phase error model correction (identifier "POD + NOPMC") and the orbits obtained by POD with mean value correction of phase error model (identifier "POD + MVC"), respectively, which can be used to obtain the improvement of POD with phase model correction. In external quality metric, the orbits computed in this paper are compared with the JPL precise science orbits (identifier "JPL"), which shows the consistency with JPL precise science orbits. JPL precise

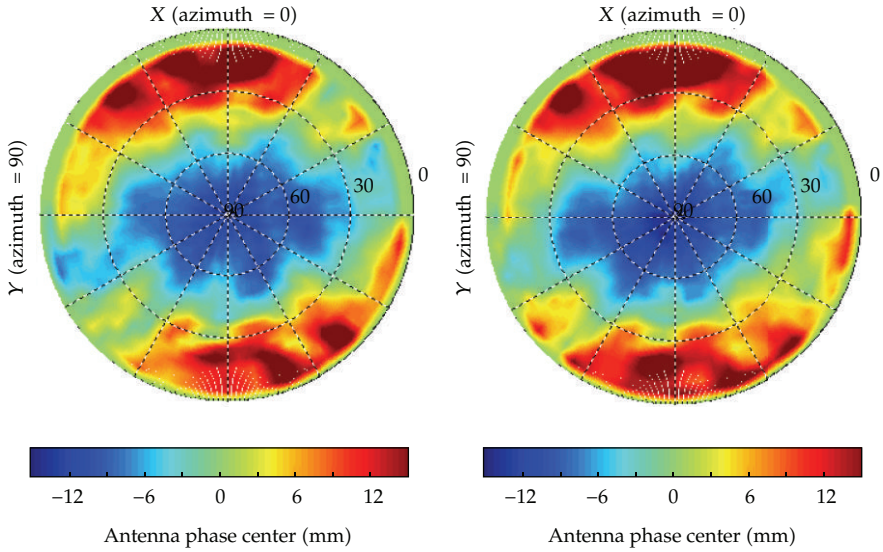

(a) Mean value pattern of phase postfit residuals of GRACE A

(b) Mean value pattern of phase postfit residuals of GRACE B

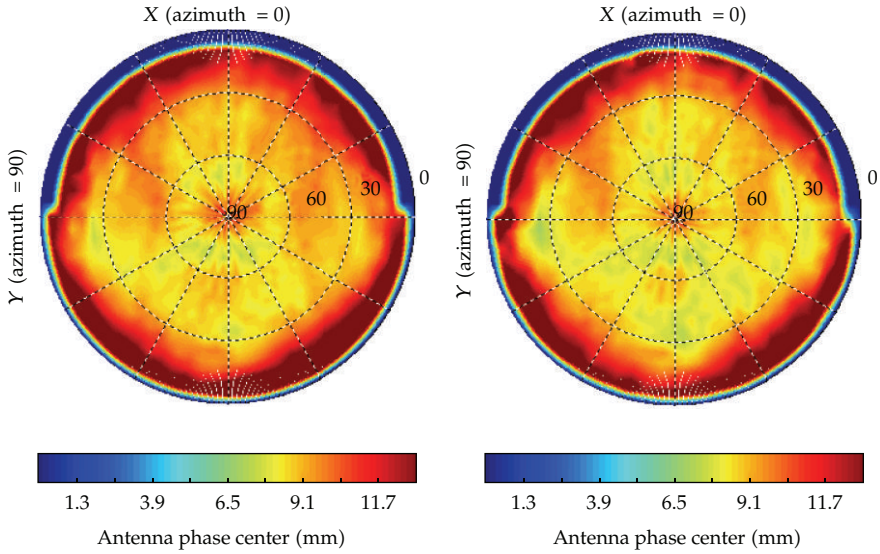

(c) Standard deviation pattern of phase postfit residuals of GRACE A

(d) Standard deviation pattern of phase postfit residuals of GRACE B

Figure 2: Mean value patterns and standard deviation patterns of phase postfit residuals of GRACE satellites.

science orbits represent one of highest precision of GRACE orbit solutions and are created by processing zero-difference ionosphere-free pseudo code and carrier phase data with the GIPSY-OASIS software package, which are distributed along with the GRACE GPS data as a part of GRACE Level 1B product. The RMS values of orbit comparisons computed in R, T, and N direction and 3D (see Figure 4) are listed in Table 5.

It is shown by the results of internal quality metric that the 3D orbit improvements arisen from phase error model correction for GRACE A and GRACE B are 0.0153 m and

Table 4: RMS values of ionosphere-free phase post-fit residuals of orbit determination.

	POD without phase error model correction/mm	POD with mean value correction of phase error model/mm	POD with phase error model correction/mm
GRACE A	12.79	9.99	9.96
GRACE B	12.27	9.46	9.28

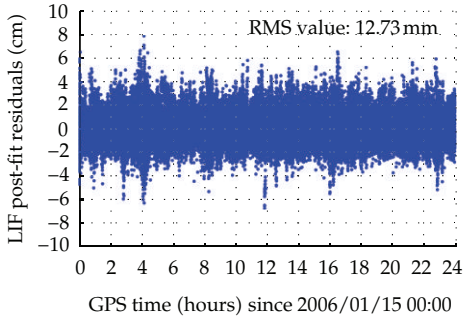

(a) Ionosphere-free phase postfit residuals of POD without phase error model correction for GRACE A on January 15, 2006

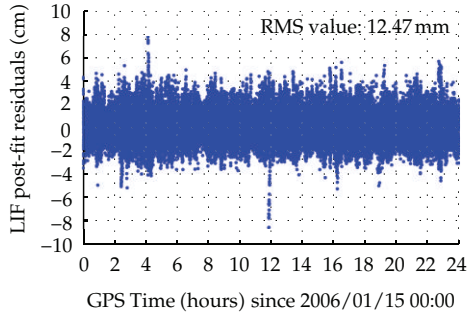

(b) Ionosphere-free phase postfit residuals of POD without phase error model correction for GRACE B on January 15, 2006

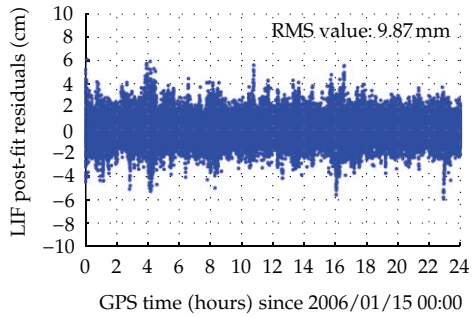

(c) Ionosphere-free phase postfit residuals of POD with mean value correction of phase error model for GRACE A on January 15, 2006

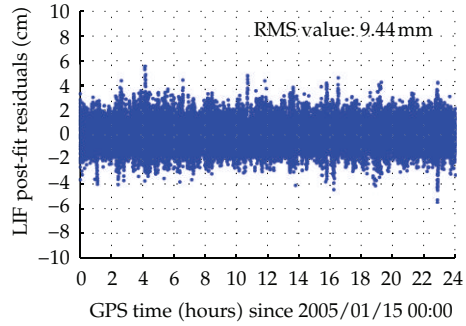

(d) Ionosphere-free phase postfit residuals of POD with mean value correction of phase error model for GRACE B on January 15, 2006

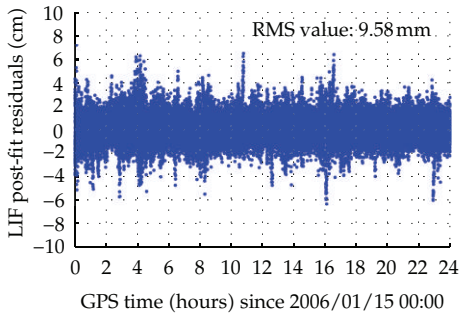

(e) Ionosphere-free phase postfit residuals of POD with phase error model correction for GRACE A on January 15, 2006

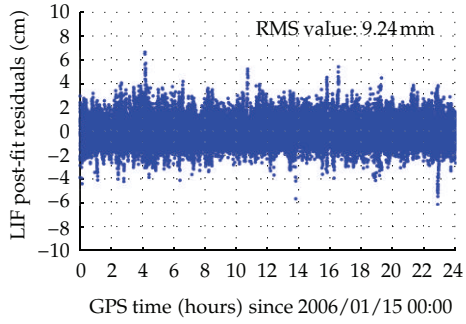

(f) Ionosphere-free phase postfit residuals of POD with phase error model correction for GRACE B on January 15, 2006

Figure 3: Ionosphere-free phase postfit residuals of orbit determination for GRACE satellites on January 15, 2006.

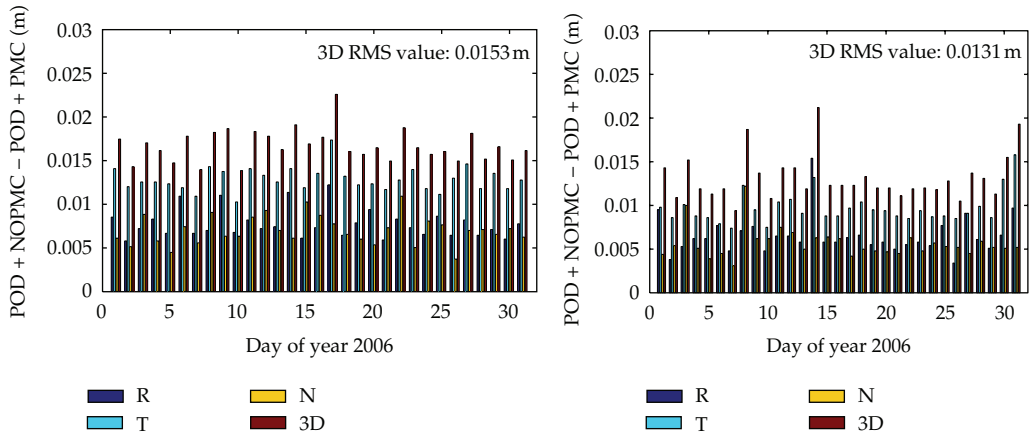

(a) POD + NOPMC – POD + PMC (GRACE A)

(b) POD + NOPMC – POD + PMC (GRACE B)

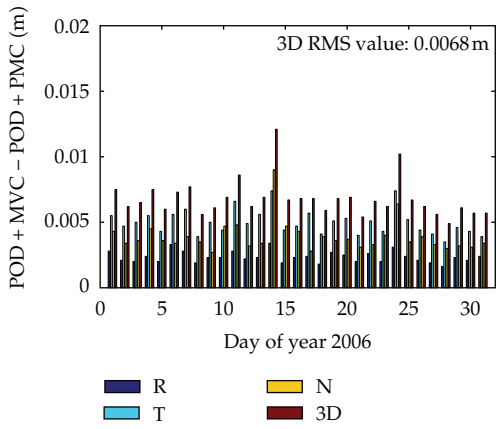

(c) POD + MVC – POD + PMC (GRACE A)

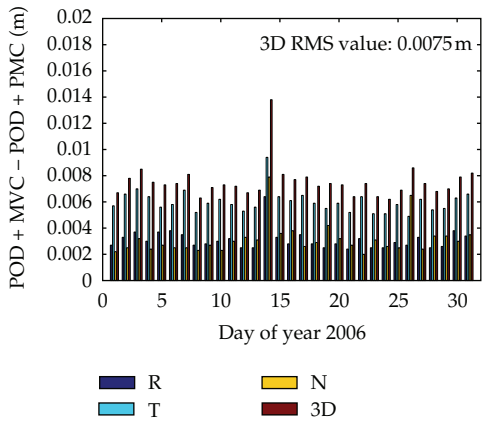

(d) POD + MVC – POD + PMC (GRACE B)

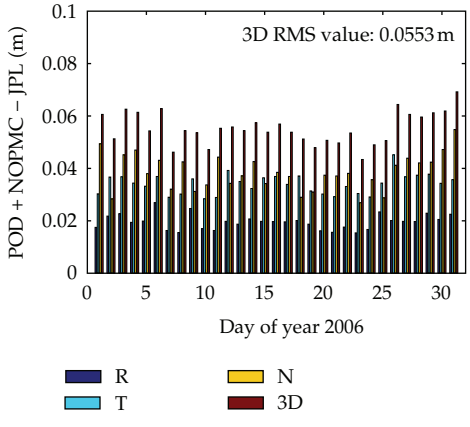

(e) POD + NOPMC – JPL (GRACE A)

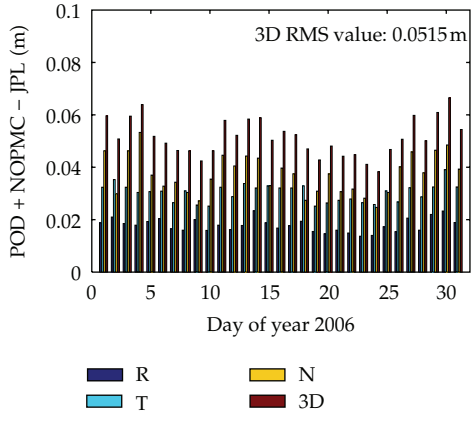

(f) POD + NOPMC – JPL (GRACE B)

Figure 4: Continued.

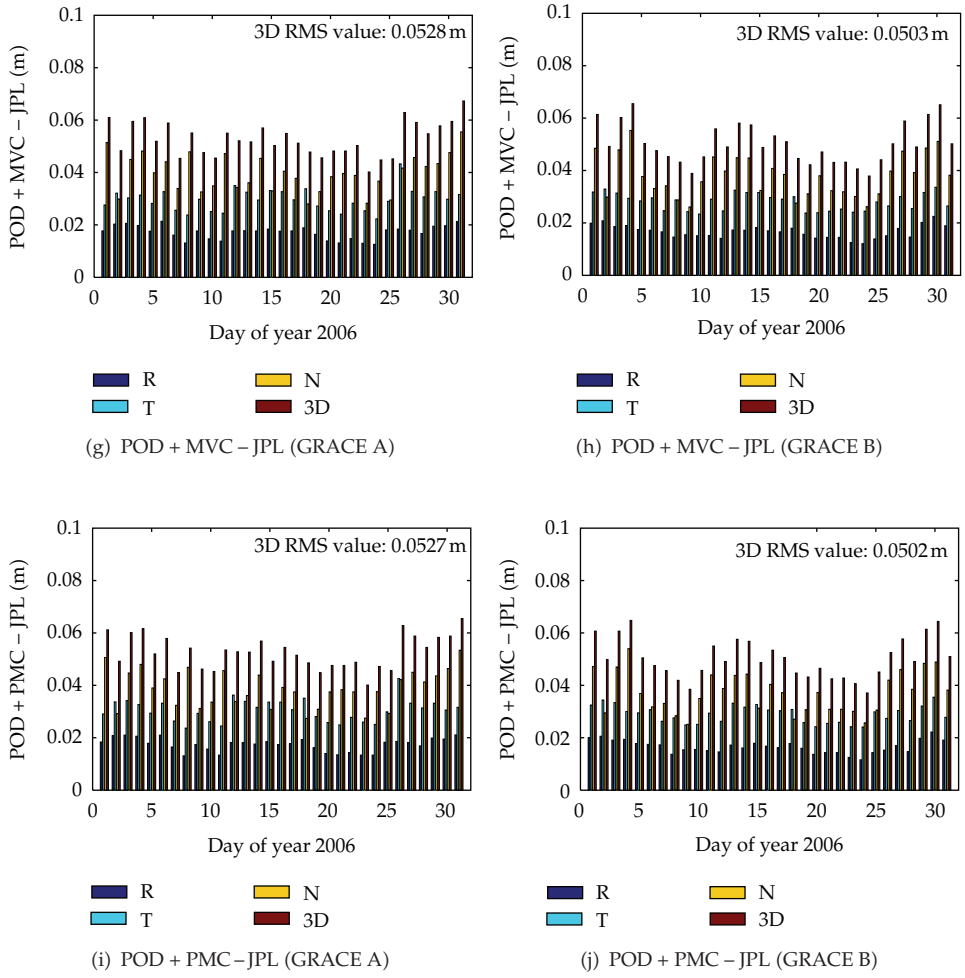

Figure 4: Orbit comparison results for GRACE A ((a), (c), (e), (g), and (i)) and GRACE B ((b), (d), (f), (h), and (j)).

0.0131 m, respectively. The most improvements are all in T direction, 0.0118 m and 0.0097 m, which is because T direction corresponds to flight direction, the phase error perpendicular to the flight direction are to some extent absorbed by the carrier phase ambiguities and clock offset, but the phase error along the flight direction will almost be absorbed by orbit parameters in orbit determination. In addition, the comparisons between the orbits derived from POD with mean value correction of phase error model and POD with phase error model correction reflect the influence arisen from random part of phase error model, and the 3D RMS values for GRACE A and GRACE B are 0.0068 m and 0.0075 m, respectively. Therefore, the random part of phase error model cannot be neglected for POD.

In external quality metric, the 3D RMS values of orbit comparison results are reduced from 0.0553 m to 0.0527 m for GRACE A and from 0.0515 m to 0.0502 m for GRACE B by POD with phase error model correction. These are slightly better than the comparison results between the orbits derived from POD with mean value correction of phase error model and

Table 5: Orbit comparison results of GRACE satellites.

Satellite	Type of orbit comparison	RMS value (m)			
		R	*T*	*N*	3D
GRACE A	POD + NOPMC – POD + PMC	0.0071	0.0118	0.0064	0.0153
	POD + PMC – POD + MVC	0.0023	0.0050	0.0039	0.0068
	POD + NOPMC – JPL	0.0195	0.0341	0.0385	0.0553
	POD + MVC – JPL	0.0172	0.0297	0.0397	0.0528
	POD + PMC – JPL	0.0174	0.0306	0.0388	0.0527
GRACE B	POD + NOPMC – POD + NOPMC	0.0065	0.0097	0.0057	0.0131
	POD + PMC – POD + MVC	0.0031	0.0060	0.0032	0.0075
	POD + NOPMC – JPL	0.0179	0.0303	0.0373	0.0515
	POD + MVC – JPL	0.0166	0.0281	0.0379	0.0503
	POD + PMC – JPL	0.0165	0.0290	0.0372	0.0502

JPL precise science orbits. It demonstrates that orbits computed by POD with phase error model correction have the higher consistency with JPL precise science orbits.

3.3.3. Orbit Validation with KBR Data

KBR system is one of the key scientific instruments onboard the GRACE satellites, which measures the one-way range change between the twin GRACE satellites with a precision of about 10 μm for KBR range at a 5-second data interval. Due to the high precision of KBR data, the relative position accuracy of the GRACE satellites can be validated. The relative positions computed by POD without phase error model correction, POD with mean value correction of phase error model, POD with phase error model correction, and JPL precise scientific orbits are validated by KBR data, respectively, (see Figure 5), and the average standard deviations of KBR comparison residuals are shown in Table 6.

From Figure 5 and Table 6, we can see that the average K-band standard deviation of the relative positions computed by POD results with phase error model correction is the least of all three types of GRACE orbit solutions generated in this paper. In addition, it is also less than the average K-band standard deviation of the relative positions computed by JPL precise science orbits. These results show that phase error model correction could remove the phase errors of both satellites and relative position accuracy could be obviously improved.

4. Conclusions

The phase error model has been set up and its model parameters have been estimated. The impact of phase error modeling on GRACE POD has been analyzed. The following conclusions are drawn from above results and discussions.

The whole phase error model is set up. The phase error is modeled as a systematic and a random component each depending on azimuth and elevation of signal reception in AFCS. The systematic part and standard deviation of random part in phase error model can both be estimated by the bin-wise mean and standard deviation values of phase postfit residuals obtained by direct orbit determination. By removing the systematic part and adjusting the weight of phase observation data according to standard deviation of random part, it leads to improved orbit parameters in a POD procedure.

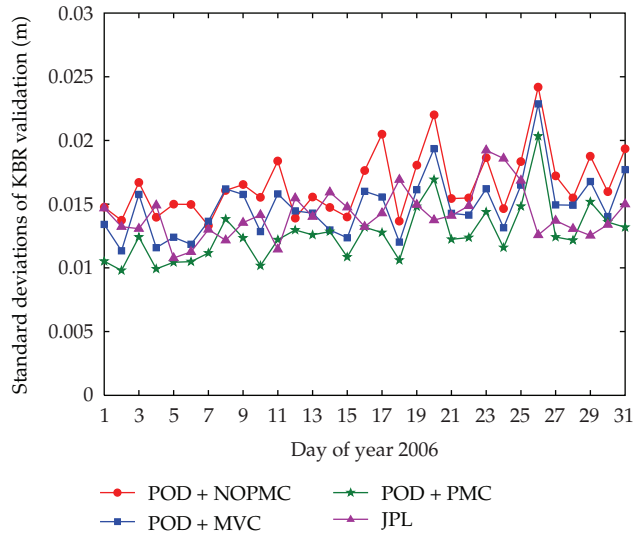

Figure 5: Daily standard deviations of KBR validation for GRACE satellites.

Table 6: Average standard deviations of KBR comparison residuals of GRACE relative position.

Type of orbit solution	Average standard deviation (m)
POD + NOPMC	0.0165
POD + MVC	0.0148
POD + PMC	0.0127
JPL	0.0142

The 31-day GRACE data of January 2006 are processed, and three types of GRACE orbit solutions by POD without phase error model correction, POD with mean value correction of phase error model, and POD with phase error model correction are generated. The impact of phase error modeling on LEO POD is analyzed by a number of tests, including phase postfit residual analysis, orbit comparison, and orbit validation with KBR data, respectively. At first, the phase postfit residual analysis shows that the RMS values of ionosphere-free phase postfit residuals of GRACE satellites derived from POD with phase error model correction are the least in the three types GRACE orbit solutions, and the applied models are in the best consistency with GPS observation data. Secondly, two quality metrics, the internal and the external, are used for orbit comparisons. In the internal metric, the 3D orbit improvements derived from phase error model correction for GRACE A and GRACE B are 0.0153 m and 0.0131 m, and the 3D influences arisen from random part of phase error model are 0.0068 m and 0.0075 m for GRACE A and GRACE B, respectively. As a result, the random part of phase error model cannot be neglected for POD. From the external quality metric, the 3D RMS values of orbit comparison residuals between the orbits computed by POD with phase error model correction and JPL precise science orbits are 0.0527 m for GRACE A and 0.0502 m for GRACE B, which are also better than another two types of orbit solutions. It shows that the orbit solutions of GRACE satellites with phase error model correction are in higher consistency with JPL precise science orbits. At last, the average K-band standard deviation of the relative positions computed by POD results with phase error

model correction is the least of all three types of GRACE orbit solutions generated in this paper, and it is also better than that derived from JPL precise science orbits.

As the aforementioned, the phase error modeling is helpful to improve precision of orbit determination, and the phase error in GPS phase observation data can be reduced. This research will have some theoretical and engineering significance on phase error correction of LEO POD.

Acknowledgments

The authors are grateful to GeoForschungsZentrum (GFZ) for providing GPS observation data, attitude data, KBR data, and precise science orbit data of GRACE mission. The authors are grateful to the Center for Orbit Determination in Europe (CODE) for providing GPS orbit solutions and clock corrections. This study is supported by the National Natural Science Foundation of China (Grant no. 61002033 and no. 60902089) and Open Research Fund of State Key Laboratory of Astronautic Dynamics of China (Grant no. 2011ADL-DW0103).

References

[1] C. Reigber, H. Lühr, and P. Schwintzer, "CHAMP mission status," *Advances in Space Research*, vol. 30, no. 2, pp. 129–134, 2002.

[2] J. van den IJssel, P. Visser, and E. Patiño Rodriguez, "CHAMP precise orbit determination using GPS data," *Advances in Space Research*, vol. 31, no. 8, pp. 1889–1895, 2003.

[3] Z. G. Kang, B. Tapley, S. Bettadpur, J. Ries, P. Nagel, and R. Pastor, "Precise orbit determination for the GRACE mission using only GPS data," *Journal of Geodesy*, vol. 80, no. 6, pp. 322–331, 2006.

[4] H. Bock, A. Jäggi, D. Švehla, G. Beutler, U. Hugentobler, and P. Visser, "Precise orbit determination for the GOCE satellite using GPS," *Advances in Space Research*, vol. 39, no. 10, pp. 1638–1647, 2007.

[5] J. H. González, M. Bachmann, G. Krieger, and H. Fiedler, "Development of the TanDEM-X calibration concept: analysis of systematic errors," *IEEE Transactions on Geoscience and Remote Sensing*, vol. 48, no. 2, pp. 716–726, 2010.

[6] O. Montenbruck and P. Ramos-Bosch, "Precision real-time navigation of LEO satellites using global positioning system measurements," *GPS Solutions*, vol. 12, no. 3, pp. 187–198, 2008.

[7] A. Jäggi, R. Dach, O. Montenbruck, U. Hugentobler, H. Bock, and G. Beutler, "Phase center modeling for LEO GPS receiver antennas and its impact on precise orbit determination," *Journal of Geodesy*, vol. 83, no. 12, pp. 1145–1162, 2009.

[8] O. Montenbruck, T. van Helleputte, R. Kroes, and E. Gill, "Reduced dynamic orbit determination using GPS code and carrier measurements," *Aerospace Science and Technology*, vol. 9, no. 3, pp. 261–271, 2005.

[9] S. Wu, T. Yunck, and C. Thornton, "Reduced-dynamic technique for precise orbit determination of low earth satellites," *Journal of Guidance Control and Dynamics*, vol. 14, no. 1, pp. 24–30, 1991.

[10] G. Beutler, A. Jäggi, U. Hugentobler, and L. Mervart, "Efficient satellite orbit modelling using pseudo-stochastic parameters," *Journal of Geodesy*, vol. 80, no. 7, pp. 353–372, 2006.

[11] J. M. Dow, R. E. Neilan, and G. Gendt, "The International GPS Service: celebrating the 10th anniversary and looking to the next decade," *Advances in Space Research*, vol. 36, no. 3, pp. 320–326, 2005.

[12] B. Haines, Y. Bar-Sever, W. Bertiger, S. Desai, and P. Willis, "One-centimeter orbit determination for Jason-1: new GPS-based strategies," *Marine Geodesy*, vol. 27, no. 1-2, pp. 299–318, 2004.

[13] B. Haines, Y. Bar-Sever, W. Bertiger et al., "Space-based satellite antenna maps, impact of different satellite antenna maps on LEO & terrestrial results," in *Proceedings of the IGS Workshop*, Miami, Fla, USA, 2008.

[14] O. Montenbruck, M. Garcia-Fernandez, Y. Yoon, S. Schön, and A. Jäggi, "Antenna phase center calibration for precise positioning of LEO satellites," *GPS Solutions*, vol. 13, no. 1, pp. 23–34, 2009.

[15] H. Bock, A. Jäggi, U. Meyer, R. Dach, and G. Beutler, "Impact of GPS antenna phase center variations on precise orbits of the GOCE satellite," *Advances in Space Research*, vol. 47, no. 11, pp. 1885–1893, 2011.

[16] D. F. Gu, *The spatial states measurement and estimation of distributed InSAR satellite system [Ph.D. thesis]*, National University of Defense Technology, Changsha, China, 2009.
[17] K. Case, G. Kruizinga, and S. Wu, *GRACE Level 1B Data Product User Handbook (Version 1. 3)*, Jet Propulsion Laboratory, Pasadena, Calif, USA, 2010.
[18] R. Dach, E. Brockmann, S. Schaer et al., "GNSS processing at CODE: status report," *Journal of Geodesy*, vol. 83, no. 3-4, pp. 353–365, 2009.
[19] R. Kroes, *Precise relative positioning of formation flying spacecraft using GPS [Ph.D. thesis]*, Delft University of Technology, Delft, The Netherlands, 2006.
[20] B. Tapley, J. Ries, S. Bettadpur et al., "GGM02—an improved Earth gravity field model from GRACE," *Journal of Geodesy*, vol. 79, no. 8, pp. 467–478, 2005.
[21] D. D. McCarthy, "IERS conventions 1996," IERS Technical Note 21, Observatoire de Paris, Paris, France, 1996.
[22] O. Montenbruck and E. Gill, *Satellite Orbits*, Springer, Heidelberg, Germany, 2000.
[23] R. Ferland, "ITRF coordinator report," 2000 IGS Annual Report, Jet Propulsion Laboratory, Pasadena, Calif, USA, 2001.
[24] D. McCarthy and G. Petit, "IERS conventions 2003," IERS Technical Note 32, Observetoire de Paris, Paris, France, 2004.
[25] D. J. Peng and B. Wu, "Zero-difference and single-difference precise orbit determination for LEO using GPS," *Chinese Science Bulletin*, vol. 52, no. 15, pp. 2024–2030, 2007.
[26] T. Y. Huang and Q. L. Zhou, "Adams-Cowell integrator with a first sum," *Chinese Astronomy and Astrophysics*, vol. 17, no. 2, pp. 205–213, 1993.